Supporting Information

Shansi Wei [a], Dai Li [a], Manqi Zang [b], Huajie Chen [a], Fengyuan Yong [a], Jiaqing Zhang [a], Huiyun Wen [a], Weiming Xue [a], Lipeng Zhang [c, *], and Saipeng Huang [a, *]

[*] Corresponding authors.

[a] School of Chemical Engineering, Northwest University, Xi’ an, PR China

[b] Sino-Germany College of Science and Technology，Qingdao University of Science and Technology, Qingdao 266042, PR China

[c] Shandong Academy of Chemical Technology, Qingdao University of Science and Technology, Jinan 250014, PR China. E-mail:lipzhang@qust.edu.cn

Lipeng Zhang (e-mail): lipzhang@qust.edu.cn

Saipeng Huang (e-mail): huangsaipeng@nwu.edu.cn

Experimental section

Text S1

1. Chemicals and reagents

All chemicals in this research are analytical pure and received without further purification to ensure consistency in all experimental conditions. Vitamin B12 ($C_{63}H_{88}CoN_{14}O_{14}P$, ≥98 %), L-Try (≥98 %), $NaNO_2$ (≥98 %), H_2O_2 (≥30 %), ethanol (≥99.5 %), anhydrous CH3COONa (NaAc, ≥99 %) and CH3COOH (HAc, ≥99 %), 3, 3′, 5, 5′-Tetramethylbenzidine (TMB) (≥98 %), Metal salts ($MgCl_2$, $BaCl_2$, $CuSO_4$, $MnCl_2$, $Pb(NO_3)_2$, KCl, $CaCl_2$, NaF, Na_2Ac, Na_2CO_3, $NaNO_3$, NaCl, Na_2SO_4), and Sodium bisulfite ($NaHSO_3$) were procured from Aladdin Reagent Co., Ltd (Shanghai, China) with a guaranteed purity of ≥98%. L-glutathione (GSH) was acquired from Shanghai Titan Scientific Co., Ltd. (Shanghai, China). Glucose (Glu) and potassium iodide (KI) were purchased from Tianjin Damao Chemical Reagent Partnership Enterprise (Limited Partnership). L-cysteine (L-cy) was purchased from InnoChem Co., Ltd. (Beijing, China). Ascorbic acid (AsA) was procured from Shanghai Zhanyun Chemical Co., Ltd. LB agar powders were provided by Sigma Aldrich (Shanghai, China). All ultrapure water were obtained from MilliQ water purifier for sample dissolution.

2. Instrumentation and Characterization

Ultraviolet-visible absorption spectra were recorded by Shimazu UV-2600 spectrophotometer. The fluorescence spectra of Co-CDs were recorded by F-970 fluorescence spectrophotometer (Shanghai, China) with a scan rate of 1200 nm·min-1, excitation and emission slit widths of 5 nm and 2.5 nm, and excitation (Ex)/emission wavelength (Em) of 374 nm and 444 nm, respectively. The FD-1-50 Vacuum Freeze Dryer from Beijing Boyikang Laboratory Instruments removed solvents from active samples. It freezed the sample, then reduced the surrounding pressure and applied controlled heat, causing the frozen solvent to sublimate directly from the solid state to the gas phase. Core components include a vacuum pump, a condensation chamber

(cold trap) to capture sublimated vapors, and temperature-controlled shelves. This equipment was used to prepare Co-CDs powders for subsequent storage. Fourier-transform infrared spectroscopy (FT-IR) analysis was performed by Frontier PerkinElmer FT-IR spectrometer with a wavenumber range of 4000 to 400 cm^{-1}. Transmission electron microscopic (TEM) and high-resolution TEM (HRTEM) images were photographed by JEM 2100 microscopes (JEOL, Japan) at the acceleration voltage of 200 kV. The crystallographic structure of Co-CDs powder was analyzed by X-ray diffraction (XRD) Bruker D8 Advance instrument. X-ray photoelectron spectroscopy (XPS) was conducted by X-ray spectrometer (Thermo Escalab 250xi, Thermo Fisher Scientific, USA) by an AlKα excitation X-ray source (1487.2 eV) with X-ray spot of 650 μm. Electron paramagnetic resonance (EPR) spectroscopy on a Bruker EMX PLUS instrument (Germany) was applied to identify superoxide radical signal, utilizing 5, 5-dimethyl-1-pyrroline n-oxide (DMPO) as spin trapping reagent. All visualized images of Co-CDs were taken and photographed by smartphone (iphone 13).

3. Steady-state kinetic assays of Co-CDs

The kinetics performance of Co-CDs was investigated by colorimetric assay utilizing TMB as the chromogenic substance to evaluate peroxidase-like characteristic. Different concentrations of H_2O_2 (0.05-3.5 mM) or TMB (0.1-0.4 mM) were transferred into 100 μL Co-CDs (200 $\mu g \cdot mL^{-1}$) in acetate buffer (pH=3.6). All samples were incubated at 20°C under continuous stirring for 30 min. Finally, the absorbency of oxidized TMB (oxTMB) was captured at 652 nm and the molar extinction coefficient (ε) of oxTMB was determined as 39,000.

$$V = \frac{V_{mas} \times [S]}{K_m + [S]}$$

Where V represents the initial beginning reaction rate of enzyme, [S] denotes the substrate concentration, Vmax is the maximum reaction rate, reflecting the enzyme's catalytic activity and efficiency, and Km is the Michaelis constant, indicating the enzyme-substrate affinity.

In this equation, V can be calculated from the absorbance of oxTMB at 652 nm

according to Lambert-Beer's rule. In addition, Vmax and Km values can be plotted from the Lineweaver-Burk reciprocal curve and calculated based on the related curve parameters.

$$\frac{1}{V} = \frac{K_m}{V_{max}} \times \frac{1}{[S]} + \frac{1}{V_{max}}$$

4. Visualization determination of NO_2^- by smartphone

Smartphone-based colorimetric assay was utilized to realize precise and quantitative measurement of NO_2^-. The RGB value was constructed to evaluate the accurate color variation by F-Color picker software of smartphone. Sulfur ion with different concentrations were added to 4mL mixed system，including sodium acetate buffer (pH = 3.6), Co-CDs (200 μg·mL^{-1}), H_2O_2 (0.25 mM) and TMB (0.35 mM). After incubation for 5 min, the optical recognition App on a smartphone was utilized to scan and capture the color changes to obtain quantitative data, which was subsequently converted to the corresponding RGB value. Finally, the linear relationship between R value and NO_2^- concentration was fitted to achieve convenient and quantitative detection. All images are taken and photographed by iphone13.

5. Detection of NO_2^- in actual samples

To explore specific application in real samples, Co-CDs towards NO_2^- detection was verified by ponds，tap and pickles water as practical samples, which were collected at Northwest University. Water samples (ponds，tap and pickles water) were centrifuged (8000 rpm, 10 min) and filtered by 0.22 μm filter membrane, which was added with NO_2^- in standard concentrations. Based on the linear range, spiked recovery tests were performed at low, medium, and high concentrations (10, 20, and 30 μM). The absorbance of sample was detected at 452 nm, which was utilized to calculate and analyze NO_2^- concentrations based on the linear fitting equation.

Text S2

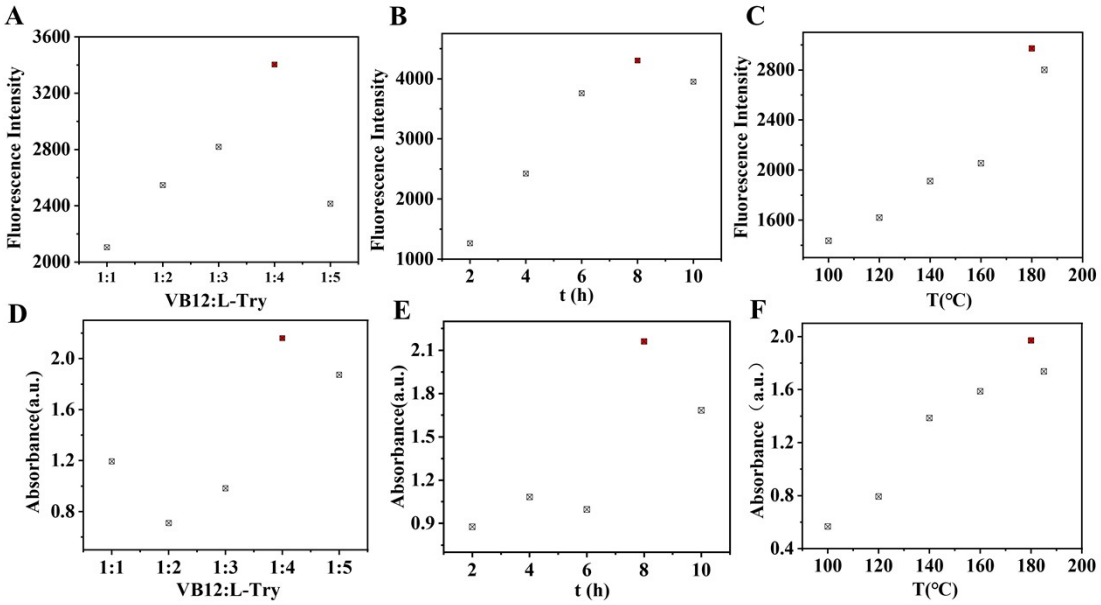

Fig. S1 Optimization of synthesis conditions for Co-CDs by fluorescence detection: (A) ratio, (B) time, (C) temperature and the peroxidase activity of Co-CDs was optimized by ratio (D)，time (E) and temperature (F).

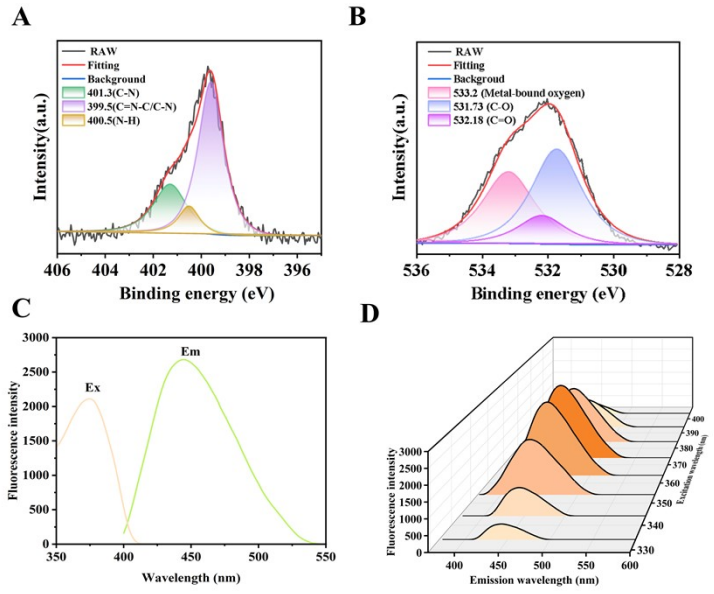

Fig. S2 HR-XPS spectra of N1s (A), O1s (B); (C) Fluorescence excitation and emission spectra of Co-CDs; (D) Fluorescence spectra of Co-CDs at different excitation wavelengths.

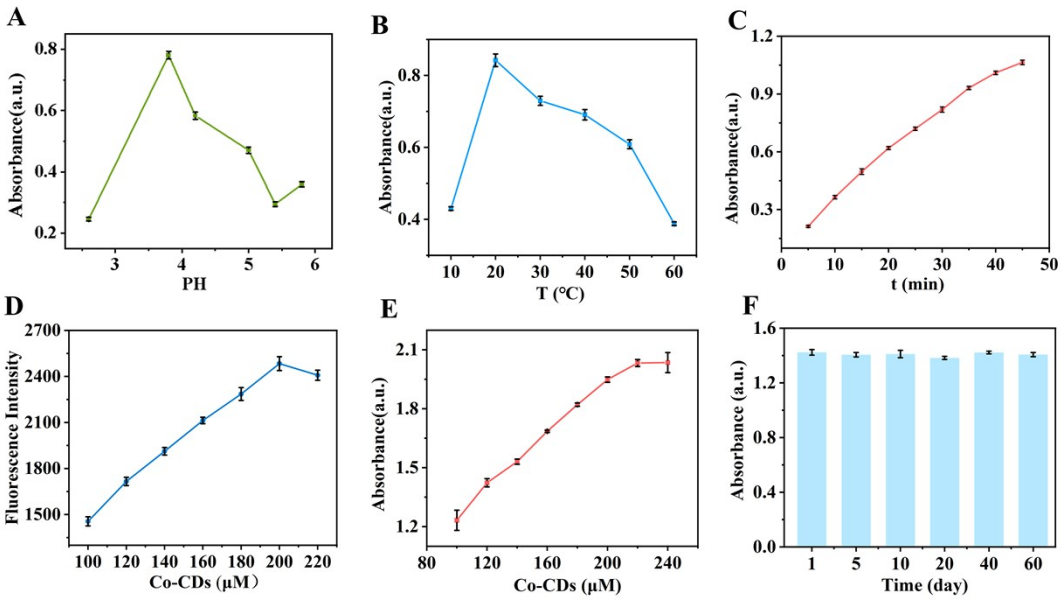

Fig. S3 The influence factor including (A) pH; (B) temperature; (C) Duration time and concentration changes on the fluorescence intensity (D) and ultraviolet absorption (E) of the reaction system; (F) Evaluation of the catalytic stability of Co-CDs at different storage times.

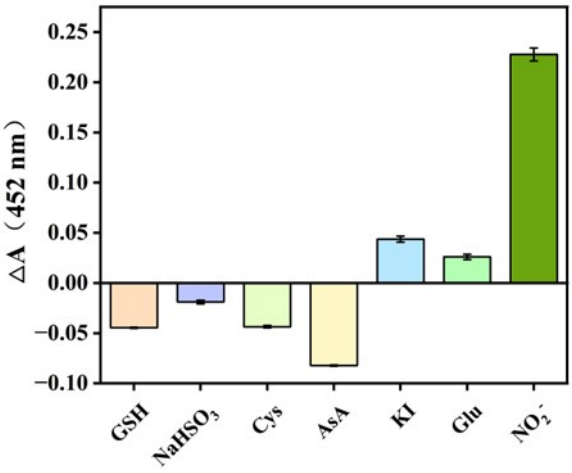

Fig. S4 UV-vis absorption (at 452 nm) change of Co-CDs after incubating with NO_2^- and other reducing substances.

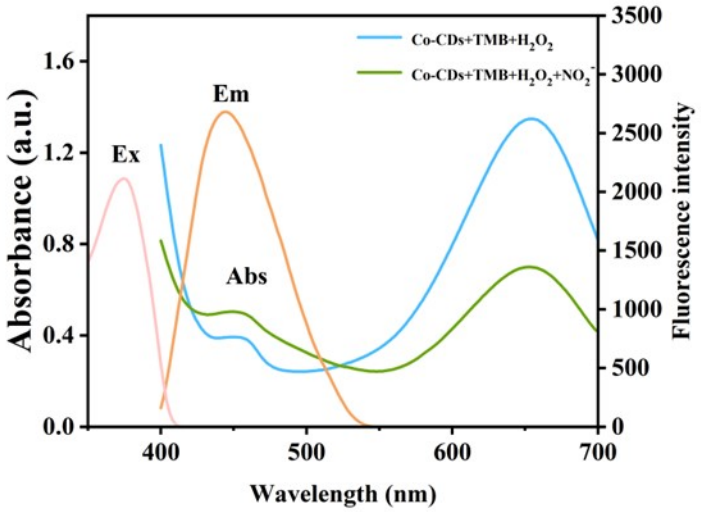

Fig. S5 The fluorescence spectra of excitation and emission of the system and the UV absorption spectra of the system before and after the addition of NO_2^-.

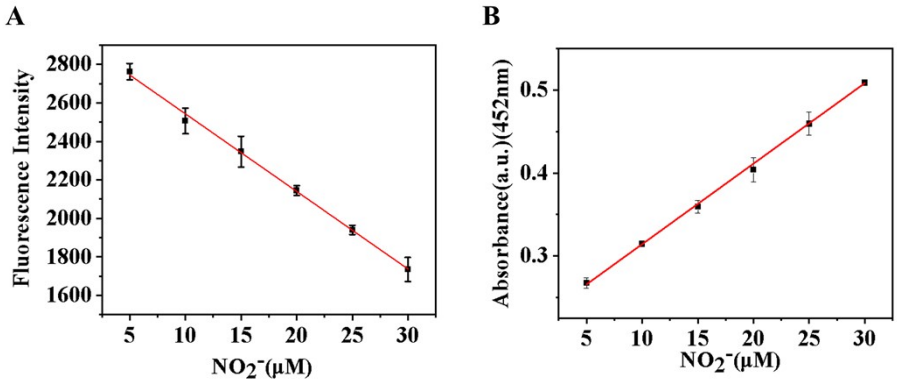

Fig. S6 The linear range of fluorescence (A) and ultraviolet detection (B) in the range of 5-30 μM NO_2^-.

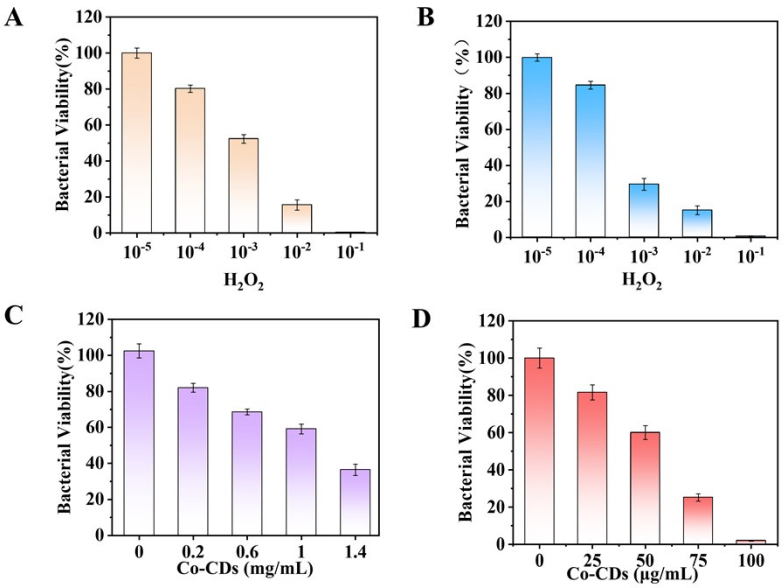

Fig. S7 Viability of S. aureus (A) and E. coli (B) with different concentrations of H_2O_2; Bacterial activity analysis under various incubation concentration of Co-CDs against S. aureus (C) and E. coli (D) (n=3);

Table S1 Steady-state kinetics of Co-CDs and other peroxidase-like mimics.

Catalysts	K_m (mM)		V_{max} (10^{-8} Ms^{-1})		Ref.
	TMB	H_2O_2	TMB	H_2O_2	
Mo-CDs	0.245	0.176	3.20	4.76	Lu et al. (2023)[1]
CDs	0.237	0.785	4.92	23.74	Dong et al. (2025)[2]
Cu-CDs	0.65139	1.9138	11.952	7.0582	Wang et al. (2024)[3]
CoNP-CDs	1.76	0.26	55.97	35.01	Nie et al. (2024)[4]
Fe-Glu	4.41	0.224	38.78	7.74	Wang et al. (2024)[5]
N-CD-Fe	0.378	0.217	84.1	110	Shi et al. (2025)[6]
FeP/CDs	0.24	175	0.84	155	Dong et al. (2024)[7]
Co-CDs	0.209	0.104	3.47	2.204	This work

1 W. Lu, Y. Guo, Y. Yue, J. Zhang, L. Fan, F. Li, Y. Zhao, C. Dong and S. Shuang, *Chem. Eng. J.*, 2023, **468**, 143615.

2 X. Dong, W. Yan, D. Zhang, X. Dong and Y. Li, *Int. J. Biol. Macromol.*, 2025, **304**, 140875.

3 Y. Wang, T. Li, L. Lin, D. Wang and L. Feng, *RSC Adv.*, 2024, **14**, 27873-27882.

4 L. Nie, S. Li, L. Jiang, L. Bu, G. Dong, D. Song, J. Liao, G. Tang and Q. Zhou, *J. Colloid Interface Sci.*, 2024, **678**, 266-276.

5 S. Wang, J. Tang, M. Liu, F. Meng, S. Wang, Y. Bai, H. Zhou and K. Du, *Food Biosci*, 2024, **62**, 105572.

6 Y. Shi, Y. Ma, L. Bao, M. Pan, M. Jiang, X. Yu and L. Xu, *BIOSENS BIOELECTRON*, 2025, **293**, 118153.

7 J. Dong, G. Liu, Y. V. Petrov, Y. Feng, D. Jia, V. E. Baulin, A. Yu Tsivadze, Y. Zhou and B. Li, *Adv. Healthcare Mater.*, 2024, **13**, 2402568.